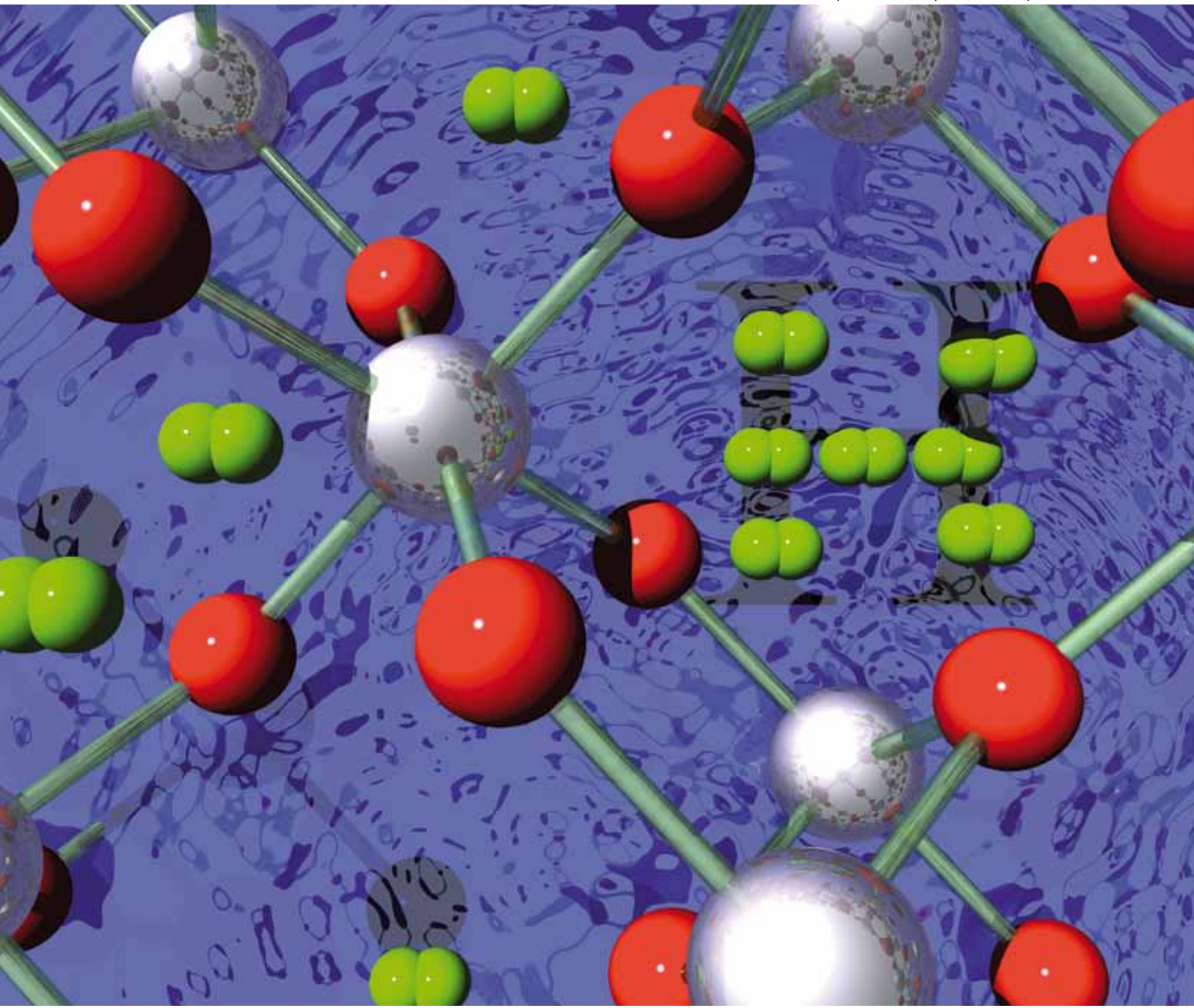


Energy & Environmental Science

www.rsc.org/ees

Volume 2 | Number 7 | July 2009 | Pages 713–804



ISSN 1754-5692

RSC Publishing

COVER ARTICLE

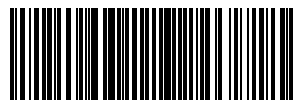
Aron Walsh *et al.*

Ternary cobalt spinel oxides for solar driven hydrogen production: Theory and experiment

REVIEW

Nigel Brandon *et al.*

Fuel cells for micro-combined heat and power generation



1754-5692(2009)2:7;1-Z

Ternary cobalt spinel oxides for solar driven hydrogen production: Theory and experiment

Aron Walsh,^{*a} Kwang-Soon Ahn,^b Sudhakar Shet,^a Muhammad N. Huda,^a Todd G. Deutsch,^a Heli Wang,^a John A. Turner,^a Su-Huai Wei,^a Yanfa Yan^a and Mowafak M. Al-Jassim^a

Received 19th December 2008, Accepted 13th March 2009

First published as an Advance Article on the web 25th March 2009

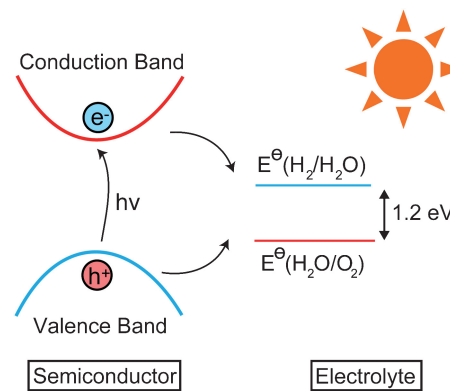
DOI: 10.1039/b822903a

Discovery of a chemically stable, light absorbing and low resistivity metal oxide with band edges aligned to the water redox potentials has been a goal of physical scientists for the past forty years. Despite an immense amount of effort, no solution has been uncovered. We present a combined theoretical and experimental exploration of a series of unconventional ternary cobalt spinel oxides, which offer chemical functionality through substitution on the octahedral spinel B site. First-principles predictions of the substitution of group 13 cations (Al, Ga, In) in Co_3O_4 to form a series of homologous CoX_2O_4 spinel compounds are combined with experimental synthesis and photoelectrochemical characterization. Ultimately, while tunable band gaps in the visible range can be obtained, the material performance is limited by poor carrier transport properties associated with small polaron carriers. Future design pathways for metal oxide exploration are discussed.

Introduction

Photoelectrochemical (PEC) decomposition of water by visible light remains the most desirable hydrogen production method for post fossil-fuel energy employment (Fig. 1).^{1,2} Metal oxide photoelectrodes are of particular interest due to their low cost and relatively high stability in aqueous media. Despite the good catalytic activity of materials such as TiO_2 ,^{3,4} oxides are generally limited by too large band gaps, which fail to absorb a significant fraction of visible light, resulting in poor solar to hydrogen conversion efficiencies under terrestrial conditions. After almost four decades of intensive research, no material has been found to simultaneously satisfy all the criteria required for widespread PEC application:^{5–9} (i) low band gap (1.7–2.2 eV), (ii) low resistivity, (iii) low cost, (iv) corrosion resistant, (v) correct alignment of band edges with respect to the water redox potentials.

The majority of PEC oxide research has centered on trying to overcome issues associated with known photoactive materials (e.g. TiO_2 , Fe_2O_3 , WO_3) through doping or alloying. However, the incremental increases in efficiency presently achieved will not be enough to make PEC based hydrogen production



^aNational Renewable Energy Laboratory, Golden, CO, 80401, USA.
E-mail: a.walsh@nrel.gov

^bSchool of Display and Chemical Engineering, Yeungnam University, Daegu, Kyungsan, 712-749, South Korea

Fig. 1 Schematic redox cycle for decomposition of water using a photoactive semiconductor.

Broader context

The efficient generation of hydrogen from water using visible light would provide a means to produce a chemical energy carrier providing current solar cell technologies with energy storage as well as providing a transportation fuel and a chemical feedstock. The conceptually simple photoelectrochemical process represents the most efficient pathway for accomplishing this goal. Light absorbed in a semiconductor photoelectrode produces electrons and holes which in turn generate H_2 and O_2 , respectively. The grand challenge is discovering the right semiconductor material which can sufficiently balance cost, stability and efficiency to make the process commercially viable. In this work, we explore a series of ternary cobalt spinel oxides, where group 13 cations (Al, Ga, In) occupy the octahedral spinel sites. We demonstrate that while good optical absorption can be obtained, the transport properties are very poor owing to the localized Co 3d states, and hence the observed photoelectrochemical activity is minimal. While this rules out this class of oxide materials (combining 3dⁿ and ns⁰ cations), we suggest a number of alternative routes for forming multiterinary oxides, which may overcome these intrinsic limitations and provide candidate photoelectrode materials in the near-term.

commercially viable. We have recently been active in developing a unified approach of material design, synthesis and characterization to explore new classes of multiterinary oxide semiconductor photoelectrodes. Similar to the way that the combination of several specific cations is required for multiterinary copper oxides to exhibit high temperature superconductivity, it is our desire to combine multiple cations based on their individual chemical and physical properties (*e.g.* structural stability, catalytic activity, light absorption) to tune the material properties for enhanced oxide PEC response.

The potential of transition metal (Fe and Co) based oxide spinels has recently been highlighted *via* initial high-throughput experimental screening by Parkinson *et al.*^{10,11} and our subsequent theoretical analysis.¹² Considering the magnitude of the band gaps alone, cobalt oxide (Co_3O_4) is too low (<1.7 eV) for direct PEC water decomposition. However, the spinel structure of Co_3O_4 contains two cation coordination environments, a four-fold tetrahedral site (A, 2^+) and a six-fold octahedral site (B, 3^+) giving the overall formula AB_2O_4 . For Co_3O_4 , the band edges are determined by a combination of the crystal field split Co 3d states on the octahedral and tetrahedral cobalt sites (Fig. 2).^{12–14} Isovalent substitution on the spinel cations sites can therefore, in principle, be used to influence both the band edge character and the magnitude of the electronic band gaps and optical absorption.

In this paper, we combine theoretical electronic structure calculations with experimental synthesis and PEC characterization to perform a comprehensive examination of how the pertinent chemical and physical properties of ternary cobalt spinels can be tailored towards those of an ideal PEC catalytic photo-electrode for solar driven hydrogen production. In particular, we explore each member of the CoX_2O_4 ($\text{X} = \text{Al, Ga, In}$) chemical series. Aluminum can be viewed as an ionic spectator in the CoAl_2O_4 lattice, which preserves overall charge neutrality, but contributes little to the density of states or optical absorption. However, the substitution of heavier group 13 cations helps reduce the electronic band gap and increase optical absorption through combination of the higher binding energy cation s states and reduced Co d-d crystal field splitting. Unfortunately, while we demonstrate that the band gaps can be tuned through a large range, the intrinsic charge transport properties result in poor PEC performance due to inefficient electron-hole extraction rates and high resistivity associated with small polaron carriers.

Finally, approaches to overcome this behavior, and future pathways for oxide material design, are discussed.

Methods

Theoretical

Calculations were performed using density functional theory (DFT)^{15,16} within a plane wave basis set as implemented in the VASP^{17,18} code. The spinel (O_{h}^7) unit cell was repeated under periodic boundary conditions to approximate an infinite solid.¹⁹ The Perdew–Burke–Ernzerhof (PBE)²⁰ exchange–correlation functional was supplemented with a Coulomb U (DFT + U) to more correctly describe the correlated nature of the Co 3d states ($U - J = 2$ eV).^{12,21} The core electrons (Co, Ga:[Ar], Al:[Ne], In:[Kr], O:[He]) were treated within the projector augmented wave (PAW) method.²² A well converged $8 \times 8 \times 8$ k -point mesh and plane wave cut-off of 500 eV were employed, with atomic forces minimized to below 1 meV \AA^{-1} . The equilibrium volumes were obtained through fitting energy–volume data to the Murnaghan equation of state.²³ Cation inversion in the spinel structure was treated *via* the special quasi-random structure method.^{24,25} The optical absorption spectra were summed over all direct valence to conduction band transitions on a denser k -point mesh ($12 \times 12 \times 12$) using the all-electron WIEN2K code²⁶ and within the random phase approximation; excitonic excitations are not considered at this level.²⁷

Experimental

$\text{Co}_1 + \delta \text{X}_2 - \delta \text{O}_4$ ($\text{X} = \text{Al, Ga, In}$) thin films were grown on Ag-coated stainless steel plates (Ag/SS) and quartz glasses for PEC measurement and optical characterization, respectively, using an RF magnetron reactive co-sputtering system. Here Ag/SS was required as the substrate, because of the high temperature oxide growth (800 °C). Two sputter guns were used for the Co-Al-O and Co-In-O syntheses, where the Co_3O_4 target was fixed and the secondary target was changed to Al and In_2O_3 for CoAl_2O_4 and CoIn_2O_4 , respectively. The Co-Ga-O films were deposited using the different amounts of Ga_2O_3 powder on the Co_3O_4 target. The distance between the sputter guns and substrate was fixed at 11 cm. The substrates were rotated during deposition for enhanced uniformity and the working pressure was 1.22 Pa. The

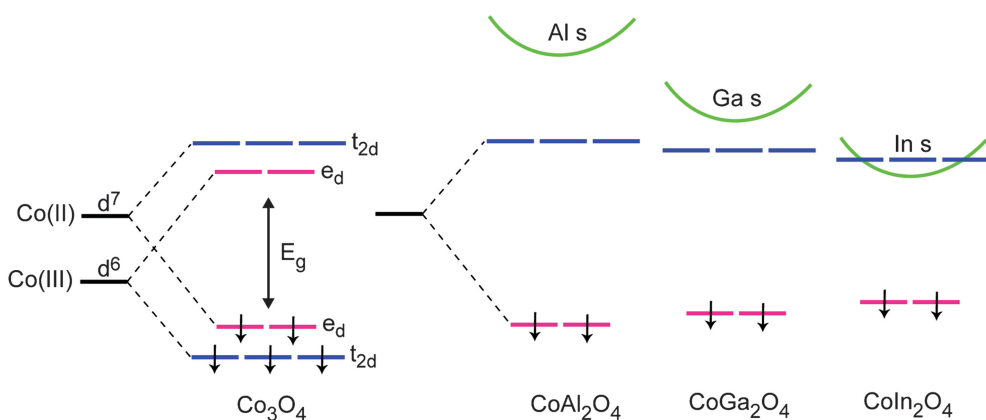


Fig. 2 Illustrated crystal field splitting of the minority spin Co 3d states in Co_3O_4 and band edge electronic structure in the ternary CoX_2O_4 ($\text{X} = \text{Al, Ga, In}$) spinels.

sputtering ambient environment was mixed Ar and O₂ (O₂:Ar = 5:1) and the RF power of each sputter gun was varied to obtain appropriate chemical stoichiometry. All of the samples were controlled to exhibit similar film thicknesses on the order of 500 nm, as measured by stylus profilometry. Structural characterization was performed by powder X-ray diffraction (XRD) measurements, using an X-ray diffractometer (XGEN-4000, SCINTAG, Inc.) operated with a Cu K α radiation source at 45 kV and 37 mA.

PEC measurements were performed in a three-electrode cell with a flat quartz window to facilitate illumination of the photoelectrode surface. The films (active area: 0.24 cm²) were used as the working electrodes. A Pt sheet (area: 10 cm²) and an Ag/AgCl electrode (with saturated KCl solution) were used as the counter and reference electrodes, respectively. A 0.5 M NaOH basic aqueous solution (pH ~ 13) was used as the electrolyte. The PEC response was measured with a fiber-optic illuminator (150 W tungsten-halogen lamp) processed through a UV/IR cut-off filter (cut-off wavelengths: 350 and 750 nm). Light intensity with the UV/IR filter was 80 mW cm⁻² as measured by a photodiode power meter. The PEC response was then measured with respect to time under chopped light on/off illumination at constant applied potential bias. Temperature effects on the dark current, due to possible sample heating on illumination, were found to be negligible.

Results

Theoretical geometric and electronic structure

Cation site preferences. The spinel crystal structure possesses two cation coordination environments: one fourfold (T_d) and two sixfold (O_h) per formula unit, Fig. 3. This introduces the possibility of cation disorder for multiterinary systems such as CoX₂O₄ (X = Al, Ga, In). The total energy difference between the normal (T_d Co and O_h X) and fully inverse structure (T_d X and random distribution of Co/X over the O_h sites), can provide an estimation of the intrinsic cation disorder for each material. CoAl₂O₄ is known to be largely normal from X-ray diffraction,²⁸

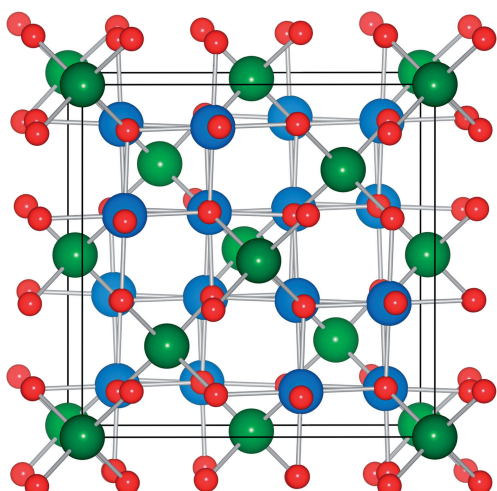


Fig. 3 Representation of the 56 atom conventional AB₂O₄ spinel unit cell with 8 T_d (A) and 16 O_h (B) cation sites colored green and blue, respectively. The 32 oxygen sites are colored red.

and this is reflected in our calculations with $\Delta E = E(\text{Inverse}) - E(\text{Normal}) = 0.51$ eV per formula unit, Table 1. For Ga and In, the inversion energy (parameter) monotonically decreases (increases) with the increased cation electronegativity. This preference for moderate disorder can also be related to the increasing ionic radii of the trivalent cations from Al to In.²⁹ As the O_h sites are stacked along ordered (111) planes in the spinel structure, partial inversion will provide beneficial strain release from the size mismatch between the Co–O and X–O bonding networks. This size difference can also be observed through the 11% increase in the calculated lattice constant between CoAl₂O₄ (8.19 Å) and CoIn₂O₄ (9.06 Å), Table 1. This corresponds to an elongation of R(Co–O) from 1.98 Å (CoAl₂O₄) to 2.05 Å (CoIn₂O₄). The decreased T_d crystal field results in a narrowing of the minimum energy Co e_d–t_{2d} separation by 0.43 eV at the Γ point on transition from Al to In. The calculated lattice constant of CoAl₂O₄ is in good agreement with the experimental value of 8.10 Å (+1%).³⁰ For CoGa₂O₄, the literature value is 8.33 Å (+2%),³¹ while for CoIn₂O₄ no structural data has been reported. The calculated formation enthalpies, between –8 and –18 eV, suggest that all compounds are thermodynamically stable.

Electronic effects. The summed local electronic density of states of each element are shown in Fig. 4. For CoAl₂O₄, the top valence band is spread between –7 to 0 eV and consists mainly of contributions from Co and O. The formal oxidation state of 2⁺ implies seven occupied 3d levels for Co. In the tetrahedral field, these are split into a fully occupied majority spin d channel (e_d²t_{2d}³) and a doubly occupied minority spin channel (e_d²t_{2d}⁰). As the Al 3s states lie to low binding energy (+3.5 eV), the electronic band gap is determined by the separation between the Co e_d and t_{2d} states in the minority spin channel. This results in a high density of states at both band edges, indicative of the underlying heavy electron and hole carrier effective masses. Replacement of Al for Ga and In maintains the same general features in the density of states; however, changes are observed, which can be related to the underlying trends in the atomic energy levels of the group 13 elements.

Firstly, Al is a row 2 element with no occupied d bands, while both Ga and In possess filled shallow core d¹⁰ levels which lie around 10 eV below their valence s states. These d states couple with O 2p and result in increased cationic contributions to the valence band, relative to Al. Secondly, the binding energies of the Ga and In s states *increase* relative to Al. Both of these effects serve to decrease the fundamental electronic band gap of the ternary cobalt oxides through enhanced anion p–cation d coupling below the valence band, and a lowering of the conduction band from the influence of the group 13 cation s states. Hence, the band gap trend observed for Al₂O₃ (8.8 eV³²), Ga₂O₃ (4.5 eV³³) and In₂O₃ (2.7 eV^{34,35}) is also maintained in the ternary cobalt oxides. Here the calculated electronic separations at the Γ point in CoX₂O₄ decrease from 2.61 (Al) to 1.70 (Ga) to 0.73 eV (In). While the quantitative reduction is overestimated due to the well-documented DFT over-binding of unoccupied cation s states, the qualitative trend remains valid. Increased dispersion is most visible in the lower conduction band density of states of CoIn₂O₄ where the conduction band minimum state is composed of majority In 5s character, which should substantially improve electron conductivity in comparison to the other ternary

Table 1 Equilibrium DFT + U structural and electronic parameters for CoX_2O_4 ($X = \text{Al}, \text{Ga}, \text{In}$), where ΔE is the energy difference between the normal and inverse spinels per formula unit, X is the associated cation disorder parameter at 300 K,²⁴ and ΔH is the formation enthalpy with respect to the elemental standard states. $E_g^{\Gamma-\Gamma}$ represents the separation between the valence and conduction bands at the Γ point

	$a_{\text{normal}}/\text{\AA}$	$a_{\text{inverse}}/\text{\AA}$	$\Delta E/\text{eV}$	$X(300\text{ K})$	$\Delta H/\text{eV}$	$E_g^{\Gamma-\Gamma}/\text{eV}$
Al	8.19	8.16	0.51	0.00	-17.56	2.61
Ga	8.46	8.43	0.23	0.02	-11.20	1.70
In	9.06	9.02	0.11	0.15	-8.05	0.73

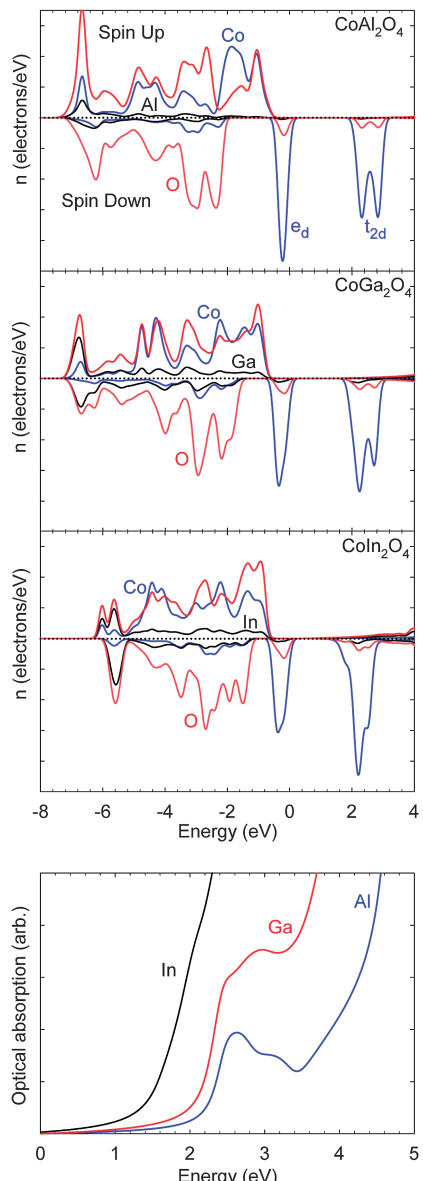


Fig. 4 Calculated local electronic densities of states and optical absorption spectra for the CoX_2O_4 ($X = \text{Al}, \text{Ga}, \text{In}$) spinel series. The highest occupied state is set to 0 eV.

oxides; however, it is unclear whether the intrinsic p-type nature of Co_3O_4 or n-type nature of In_2O_3 would dominate in the ternary composite system.

The calculated optical absorption spectra are also shown for each compound in Fig. 4. A clear redshift in the onset of

absorption is observed, consistent with the electronic band structure. For CoAl_2O_4 , the weak absorption onset is associated with low intensity $d \rightarrow d$ transitions. As the spinel lattice constant increases with the heavier group 13 cations, the splitting of the filled and empty d states is reduced and the weak absorption feature moves to lower energies. The onset of strong absorption occurring from above 3 eV in CoAl_2O_4 arises from a combination of band to band transitions composed of $p \rightarrow d$, $d \rightarrow s$ and $p \rightarrow s$ character. For CoGa_2O_4 , the energy level trends discussed above, in particular the lowering of the cation s level, result in the substantial increase in optical absorption at lower photon energies. For CoIn_2O_4 , the weak onset feature is completely lost in favour of a highly desirable sharp rise in absorption coefficient.

Experimental synthesis and characterization

The representative experimental optical data for each ternary cobalt oxide material, synthesized under a range of sputtering conditions, are shown in Fig. 5. From both the measured optical absorption coefficient and a fit to the Tauc relation for direct transitions, tailoring of the optical band gap from 1.5 to 2.25 eV can be observed. Taking into account that the separation between the $\text{H}_2/\text{H}_2\text{O}$ reduction and $\text{O}_2/\text{H}_2\text{O}$ oxidation potentials is 1.23 eV, and that due to the presence of unavoidable losses (e.g. component resistance, electron-hole recombination) an additional overpotential is required (raising the optimal voltage to ~ 1.7 eV), this optical band gap range appears quite promising for PEC water-splitting application. For CoAl_2O_4 , the measured absorption features are consistent with previous reports.^{36,37} The low energy absorption peak for CoAl_2O_4 originates from the spin allowed, parity forbidden $\text{Co } ^4\text{A}_2 \rightarrow ^4\text{T}_1$ transitions, while the drop in absorption coefficient at higher energies results from a range of low intensity spin forbidden transitions. The same general features, including the onset of strong absorption at shorter wavelengths, are observed in the calculated optical absorption spectrum (Fig. 4). The shift to longer wavelengths with lower Al sputtering power can be understood as a transition towards the inverse Co_2AlO_4 spinel, which is known to possess a lower band gap.¹² For CoGa_2O_4 , the strong absorption profile is redshifted to around 2.25 eV and begins to overlap with the low energy absorption feature; this overlap is even more pronounced for CoIn_2O_4 at high Co_3O_4 sputtering power. At high In_2O_3 sputtering power, the Co-In-O samples exhibit the high levels of visible transmission expected from mixed phase Co substituted In_2O_3 , i.e. the ternary composite is not fully formed.

The time dependant PEC response of each material was investigated under chopped light illumination at a constant applied bias potential (vs. Ag/AgCl). The cathodic currents of

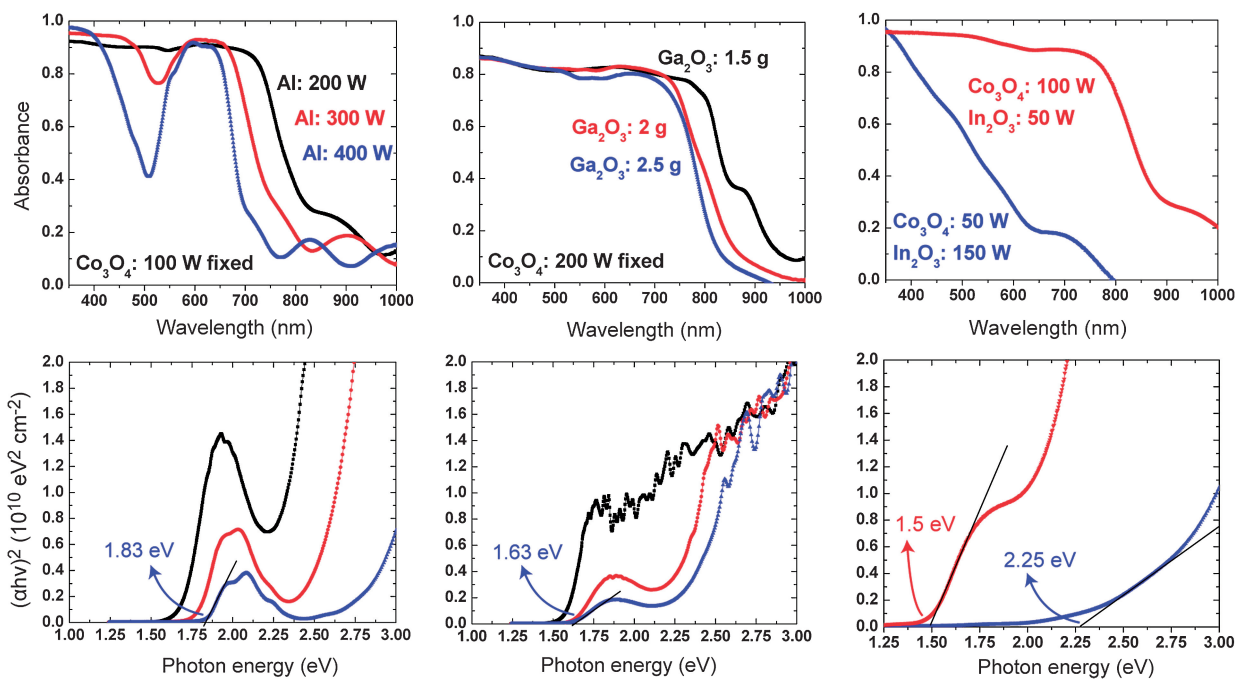


Fig. 5 Measured optical absorption spectra (upper) and direct band gap fits (lower) of $\text{Co}_1 + \delta\text{X}_2 - \delta\text{O}_4$ compounds as a function of sputtering conditions: (left) $\text{X} = \text{Al}$, (centre) $\text{X} = \text{Ga}$ and (right) $\text{X} = \text{In}$.

CoAl_2O_4 and CoGa_2O_4 were found to increase on illumination, Fig. 6. This p-type PEC response suggests the presence of intrinsic hole carriers, which prior calculations have identified as cation vacancies.³⁸ However, poor photocurrents on the order of $20 \mu\text{A cm}^{-2}$ are observed in both cases (currents on the order of 10 mA cm^{-2} will be required from commercially viable materials). It is worth noting that the PEC response of CoAl_2O_4 is better than that of CoGa_2O_4 , which will be discussed in more detail shortly. Unfortunately, all synthesized CoIn_2O_4 films failed to exhibit any significant PEC response. Indeed, the weak PEC response varied from p-type to n-type with different samples, but no significant photocurrent was observed in either case.

In addition to the low generated photocurrents, the second discouraging trend emerging from Fig. 6 is the long relaxation times between sample illumination. While for the majority of PEC materials, the recovery time on the removal of light is on the

order of seconds or less, for these materials it is on the order of minutes. This implies poor carrier transport kinetics, originating from confined electrical carriers (heavy hole effective masses). A more detailed comparison between the relaxation times of CoAl_2O_4 and CoGa_2O_4 is shown in Fig. 7. Ideally the photocurrent decay for the chopped light PEC system will follow close to a square wave; however, here the response deviates greatly. Direct comparison of the normalized current of the Al and Ga ternaries (Fig. 7), shows much faster decay in the former, indicating better carrier transport kinetics, and hence CoAl_2O_4 exhibits marginally improved PEC response. One encouraging outcome is that both materials exhibited no evidence of corrosion in solution for sustained PEC testing periods.

Based on our initial electronic structure analyses, it was anticipated that the Co-In spinel may possess both the lowest band gap and highest n-type conductivity (through the presence

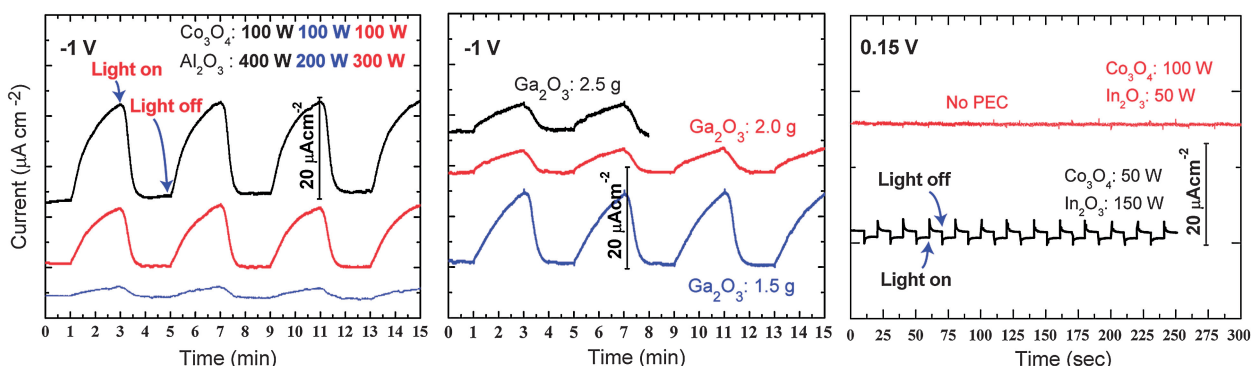


Fig. 6 Time dependant photoelectrochemical response under light on/off illumination at constant applied voltage for (left) Al, (centre) Ga and (right) In ternary cobalt oxides. For the Al and Ga spinels, illumination induces an increase in the background cathodic current (p-type response), while for In a small increase in the anodic current is observed (n-type response).

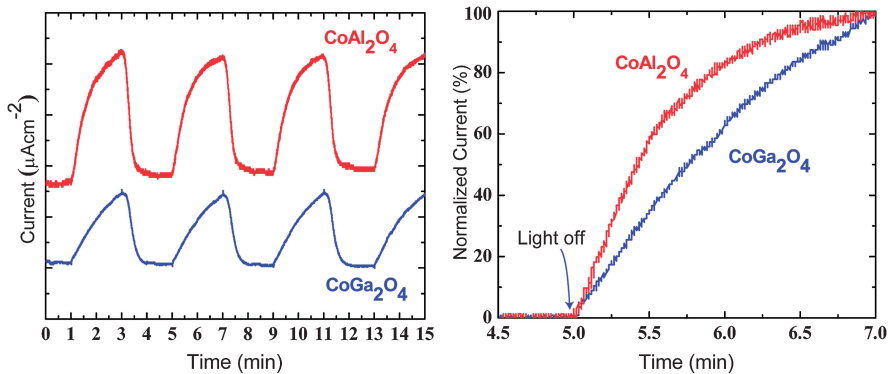


Fig. 7 Photocurrent decay comparison between the CoAl_2O_4 and CoGa_2O_4 samples with the same bias voltage (-1 V).

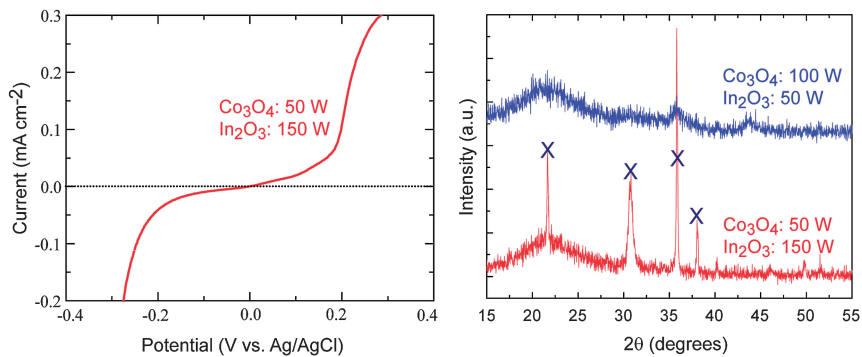


Fig. 8 Measured dark current–voltage curve and powder X-ray diffraction (XRD) data for synthesized Co–In systems. The crosses in the XRD spectrum correspond to reflections associated with bixbyite In_2O_3 .

of the In 5s conduction states). However, while the synthesized In based ternary oxides did not exhibit any significant photocurrent on illumination, the n-type PEC response time was much shorter, indicating the beneficial influence of the delocalized In 5s orbitals in the lower conduction band. To explore the origin of the performance failure in more detail, we first measured the dark currents without illumination, as shown in Fig. 8. Even for small applied potentials, the dark current is large, indicating that the film is not an intrinsic semiconductor, but is in fact closer to a semi-metallic state. The XRD curves are also shown in Fig. 8. The measurements clearly show that the deposited films are not pure CoIn_2O_4 but undergo significant phase segregation into Co_3O_4 and In_2O_3 (this has been confirmed by transmission electron microscopy analysis). Taking into account that In_2O_3 itself exhibits degenerate electron conduction behavior as an n-type transparent conducting oxide,^{39–41} the presence of In_2O_3 in the film will contribute to both the inferior PEC response and high dark current levels. Within the limitations of our co-sputtering system, we could not succeed in synthesizing a homogeneous CoIn_2O_4 film.

Discussion

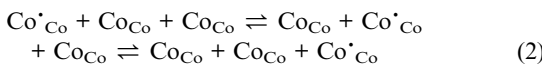
The absence of efficient water decomposition

While the prediction of tunable electronic band gaps based on density functional theory calculations was realized experimentally, the ternary cobalt samples all exhibit poor PEC

performance, which can be related to the inherent conductivity mechanisms in transition metal oxides. From examination of intrinsic point defect formation in CoAl_2O_4 , we previously identified doubly ionized cobalt vacancies as the likely source of p-type conductivity³⁸ (eqn (1), in Kröger–Vink notation⁴²), which is in agreement with early experimental observations.⁴³



Within the realm of traditional semiconductor defect theory, the generated electron holes (h^{\bullet}) are considered to behave as free carriers moving through delocalized bands. However, for conductivity in localized states (such as partially filled 3d levels), this is not the case. From a chemistry perspective, each hole formally corresponds to a net cobalt oxidation (*i.e.* $\text{h}^{\bullet} \equiv \text{Co}_{\text{Co}}^{+}$), which introduces a local lattice distortion through the contraction in the Co–O interatomic distances associated with the loss of an electron. The accessibility of the higher oxidation state (Co^{3+}) explains why these spinels favour p-type conductivity (electron deficiency). Mobility of this so-called small polaron will have an associated activation energy corresponding to the hopping of the electronic defect and associated structural distortion (eqn (2)). From a physics perspective, such polaron mediated conductivity will dominate when the electronic band width (a measure of electron delocalization in reciprocal space) of the conductive state is less than the polarization energy gained by inducing a local lattice distortion.⁴⁴ In other words, it is an effect typical of materials with heavy carrier effective masses.⁴⁵



The presence of localized carriers is detrimental for any potential semiconductor photoelectrode. The introduction of an Arrhenius-like activation energy decreases the carrier mobility by several orders of magnitude at room temperature. Furthermore, trapping of photoexcited carriers at such sites will result in an increased probability for electron–hole recombination, as well as the excessive carrier relaxation times observed in our PEC measurements for the ternary spinels.

From the reported electrical properties of single crystal CoAl_2O_4 , the conductivity is indeed characterized by an exponential rise with temperature, combined with an activation barrier on the order of 1.8 eV.⁴⁶ This results in carrier mobilities far below $1 \text{ cm}^2 \text{ V}^{-1} \text{ s}^{-1}$ and highly resistive behavior at room temperature. For Co_3O_4 , manipulation of the growth conditions has been shown to increase the conductivity by several orders of magnitude,⁴⁷ however, such an effect has not been reported in the corresponding ternary cobalt oxide compounds. The principal reason why the conductivity of the ternary spinels is diminished with respect to binary cobalt oxide, is that as the Co concentration is diluted, the Co–Co separations are increased, inducing lower hopping probabilities. Indeed, the average Co–Co separations increase by 33% from Co_3O_4 to CoIn_2O_4 , which, assuming a $1/r^2$ dependence, would result in an 89% decrease in polaron conductivity. It is worth noting that the related class of ternary ZnX_2O_4 spinels, where X = Co, Rh, Ir offer much improved p-type conductivities.⁴⁸ This is due to the presence of Co on the edge sharing spinel octahedra, which significantly lowers the barrier for polaron mobility. However, for this case, the octahedral crystal field induces a low spin Co ($t_{2g}^6e_g^0$) configuration, with optical band gaps greater than 2.3 eV, and hence they have been gaining interest for application as p-type transparent conductors.⁴⁹

One potential avenue to overcome the limitations of the CoX_2O_4 spinels is to make the materials grossly non-stoichiometric so that the cation vacancy defect levels begin to overlap, inducing a transition to band conductivity. However, such a highly defective system would not be optimal for PEC application. The only other alternatives are to further alloy with cations that can provide more dispersive character at the top of the valence band to facilitate rapid hole transport, or to employ nanoparticle or ultra thin films, where the bottleneck provided by low carrier mobility would be reduced. In particular, the application of suspended nanoparticles in a slurry phase PEC reactor, where the particle sizes are on the same order as the carrier diffusion length is a possibility for overcoming such poor transport behavior.

Moving forward

Our combined experimental and theoretical exploration has demonstrated how the fundamental properties of multicomponent oxides can be manipulated by the combination of appropriate cations. However, we have also demonstrated that serious issues exist with the inclusion of transition metal cations with localized 3d levels situated at the band edges. Indeed this is also the main limitation of Fe_2O_3 , where the good band gap and

visible light absorption are offset by inefficient photogenerated carrier separation and lackluster carrier mobility.⁵⁰ This experience can be employed as a future selection criterion in the choice of optimal cations.⁵¹

For high levels of conductivity in oxides, the dispersive conduction bands of ns^0 cations (Zn^{2+} , In^{3+} , Sn^{4+}) are highly desirable,^{39,52,53} and it has been well demonstrated in the literature that nd^0 cations (e.g. Ti^{4+} , V^{5+} , W^{6+}) can act as beneficial catalytic redox centers.^{54–57} Unfortunately, both cations tend to produce oxides with band gaps outside the visible photon range. Furthermore, it is undesirable to further lower the conduction band energy, as this will require a significant bias voltage to drive forward the hydrogen reduction reaction. It is therefore required to increase the valence band energy, which can be achieved through cation functionalization by the inclusion of cations with occupied low binding energy d or s states such as Cu/Ag (nd^{10}) or Bi/Pb (ns^2). To ensure stability in solution, it may be beneficial to also include cations which form strong metal–oxygen bonds to provide a stable structural framework in the multiterinary systems, e.g. Al, Zr, Si.

By following these intuitive design principles, we can suggest a number of potential routes for improving oxide PEC performance. An oxide class of immense current interest are the ABO_2 delafossite oxides;^{58–60} where A = Cu or Ag, and B can be any trivalent cation. While the prototype delafossite CuAlO_2 first gathered interest as a p-type transparent conductor,⁶¹ replacement of Al with alternative cations such as Cr^{62,63} can reduce the otherwise large optical band gaps and simultaneously improve the conductivity.⁶⁴ This homologous series is unique in maintaining a Cu 1^+ oxidation state; Cu containing spinels tend to induce the formation of the less desirable magnetic 2^+d^9 configuration. Similar to the ternary Co spinels presented in our current work, it should be possible to tune the band gap of the group 13 Cu delafossites through formation of the $\text{Cu}(\text{Al}_{1-x-y}\text{Ga}_x\text{In}_y)\text{O}_2$ alloy. Due to the reduced symmetry of the resulting ordered or disordered alloys, the weak band edge optical transitions associated with typical ternary delafossites⁵⁸ could be overcome.

Alternatively, post-transition metal containing oxides such as BiVO_4 have also been gathering recent attention.^{65–69} Occupied cation s states serve both to raise the valence band energy through the addition of cation s–anion p coupling^{70,71} and induce lighter hole masses than typical oxides, e.g. good p-type mobilities and conductivity have been reported in SnO .⁷² Many mineral structures combining these cations exist (e.g. ilmenite,⁷³ rosiaite⁷⁴ and trirutile⁷⁵ based compounds) and there are certainly many more complex configurations that remain to be discovered and explored. In particular, we would refer readers to recent work on bismuth technetates,⁷⁶ ternary Sn, Pb, Bi and Sb oxides,⁷⁷ and Sn based niobates and tantalates.⁷⁸ This serves to emphasize that there are many viable lines for future research beyond the PEC oxide standards such as TiO_2 .

Conclusions

We have presented a combination of theoretical electronic structure calculations with experimental synthesis and characterization of a series of ternary cobalt spinel oxides. While these materials combine excellent stability in solution and good visible light absorption properties, their performance as

photoelectrochemical catalysts is limited by the poor transport properties induced by small polaron mobility. This is an enhancement of the same effect that limits the performance of Fe_2O_3 based photocatalysts. While incremental improvements in charge carrier extraction efficiencies may be possible through the alteration and tuning of growth conditions and crystal morphology, it is unlikely that the limitations of late 3d transition metal oxides will be overcome to provide the performance required for commercial hydrogen production. We have suggested a number of potential future pathways for reducing the band gaps of metal oxides, without sacrificing electron transport performance.

Acknowledgements

We would like to thank B. A. Parkinson and M. Woodhouse for useful discussions in relation to their high throughput screening results. This work is supported by the U.S. Department of Energy (DOE) under contract no. DE-AC36-08GO28308. Computing resources of the National Energy Research Scientific Computing Center were employed, which is supported by DOE under Contract No. DE-AC02-05CH11231.

References

- M. Z. Jacobson, W. G. Colella and D. M. Golden, *Science*, 2005, **308**, 1901.
- J. A. Turner, *Science*, 1999, **285**, 687.
- A. Fujishima and K. Honda, *Nature*, 1972, **238**, 37.
- A. Fujishima, K. Kohayakawa and K. Honda, *J. Electrochem. Soc.*, 1975, **122**, 1487.
- B. D. Alexander, P. J. Kulesza, I. Rutkowska, R. Solarska and J. Augustynski, *J. Mater. Chem.*, 2008, **18**, 2298.
- T. Bak, J. Nowotny, M. Rekas and C. C. Sorrell, *Int. J. Hydrogen Energy*, 2002, **27**, 991.
- N. S. Lewis, *Nature*, 2001, **414**, 589.
- O. Khaslev and J. A. Turner, *Science*, 1998, **280**, 425.
- A. Kudo and Y. Miseki, *Chem. Soc. Rev.*, 2009, **38**, 253.
- M. Woodhouse, G. S. Herman and B. A. Parkinson, *Chem. Mater.*, 2005, **17**, 4318.
- M. Woodhouse and B. A. Parkinson, *Chem. Mater.*, 2008, **20**, 2495.
- A. Walsh, S.-H. Wei, Y. Yan, M. M. Al-Jassim, J. A. Turner, M. Woodhouse and B. A. Parkinson, *Phys. Rev. B*, 2007, **76**, 165119.
- K. M. E. Miedzinska, B. R. Hollebone and J. G. Cook, *J. Phys. Chem. Solids*, 1987, **48**, 649–656.
- Y. Jugnet and T. M. Duc, *J. Phys. Chem. Solids*, 1979, **40**, 29.
- P. Hohenberg and W. Kohn, *Phys. Rev.*, 1964, **136**, B864.
- W. Kohn and L. J. Sham, *Phys. Rev.*, 1965, **140**, A1133.
- G. Kresse and J. Furthmüller, *Comput. Mater. Sci.*, 1996, **6**, 15.
- G. Kresse and J. Furthmüller, *Phys. Rev. B*, 1996, **54**, 11169.
- M. C. Payne, M. P. Teter, D. C. Allan, T. A. Arias and J. D. Joannopoulos, *Rev. Mod. Phys.*, 1992, **64**, 1045.
- J. P. Perdew, K. Burke and M. Ernzerhof, *Phys. Rev. Lett.*, 1996, **77**, 3865.
- S. L. Dudarev, G. A. Botton, S. Y. Savrasov, C. J. Humphreys and A. P. Sutton, *Phys. Rev. B*, 1998, **57**, 1505.
- P. E. Blöchl, *Phys. Rev. B*, 1994, **50**, 17953.
- F. D. Murnaghan, *Proc. Nat. Acad. Sci. U. S. A.*, 1944, **30**, 244.
- S.-H. Wei and S. B. Zhang, *Phys. Rev. B*, 2001, **63**, 045112.
- S.-H. Wei, L. G. Ferreira, J. E. Bernard and A. Zunger, *Phys. Rev. B*, 1990, **42**, 9622.
- P. Blaha, K. Schwarz, G. K. H. Madsen, D. Kvashnicka and J. Luitz, *WIEN2k, An Augmented Plane Wave + Local Orbitals Program for Calculating Crystal Properties*, Techn. Universität Wien, Austria, 2001.
- C. Ambrosch-Draxl and J. O. Sofo, *Comput. Phys. Commun.*, 2006, **175**, 1.
- N. Tristant, J. Hemberger, A. Krimmel, H. A. K. von Nidda, V. Tsurkan and A. Loidl, *Phys. Rev. B*, 2005, **72**, 174404.
- R. D. Shannon, *Acta Crystallogr., Sect. A*, 1976, **32**, 751.
- H. Furuhashi, M. Inagaki and S. Naka, *J. Inorg. Nucl. Chem.*, 1973, **35**, 309.
- A. Nakatsuka, Y. Ikeda, N. Nakayama and T. Mizota, *Acta Crystallogr., Sect. E*, 2006, **62**, i109.
- T. Perevalov, A. Shaposhnikov, V. Gritsenko, H. Wong, J. Han and C. Kim, *JETP Lett.*, 2007, **85**, 165.
- G. Schmitz, P. Gassmann and R. Franchy, *J. Appl. Phys.*, 1998, **83**, 2533.
- A. Walsh, J. L. F. Da Silva, S.-H. Wei, C. Korber, A. Klein, L. F. J. Piper, A. DeMasi, K. E. Smith, G. Panaccione, P. Torelli, D. J. Payne, A. Bourlange and R. G. Eg dell, *Phys. Rev. Lett.*, 2008, **100**, 167402.
- A. Bourlange, D. J. Payne, R. G. Eg dell, J. S. Foord, P. P. Edwards, M. O. Jones, A. Schertel, P. J. Dobson and J. L. Hutchison, *Appl. Phys. Lett.*, 2008, **92**, 092117.
- U. Lavrenčič Štarang, B. Orel and M. Krajnc, *J. Sol-Gel Sci. Technol.*, 2003, **26**, 771–775.
- M. Zayat and D. Levy, *Chem. Mater.*, 2000, **12**, 2763.
- A. Walsh, Y. Yan, M. M. Al-Jassim and S.-H. Wei, *J. Phys. Chem. C*, 2008, **112**, 12044.
- A. Walsh, J. L. F. Da Silva and S.-H. Wei, *Phys. Rev. B*, 2008, **78**, 075211.
- C. G. Granqvist and A. Hultaker, *Thin Solid Films*, 2002, **411**, 1.
- P. D. C. King, T. D. Veal, D. J. Payne, A. Bourlange, R. G. Eg dell and C. F. McConville, *Phys. Rev. Lett.*, 2008, **101**, 116808.
- D. M. Smyth, *The Defect Chemistry of Metal Oxides*, Oxford University Press, Oxford, 2000.
- C. Greskovich and H. Schmalzried, *J. Phys. Chem. Solids*, 1970, **31**, 639.
- P. A. Cox, *The Electronic Structure and Chemistry of Solids*, Oxford University Press, New York, 1987.
- N. F. Mott and R. Peierls, *Proc. Phys. Soc., London*, 1937, **49**, 72.
- N. G. Matveeva and A. I. Shelykh, *Phys. Status Solidi B*, 1972, **50**, 83–86.
- F. Tronel, L. Guerlou-Demourgues, M. Menetrier, L. Croguennec, L. Goubault, P. Bernard and C. Delmas, *Chem. Mater.*, 2006, **18**, 5840.
- M. Dekkers, G. Rijnders and D. H. A. Blank, *Appl. Phys. Lett.*, 2007, **90**, 021903.
- H. Hosono, *Thin Solid Films*, 2007, **515**, 6000–6014.
- A. Kleiman-Shwarzstein, Y.-S. Hu, A. J. Forman, G. D. Stucky and E. W. McFarland, *J. Phys. Chem. C*, 2008, **112**, 15900.
- M. N. Huda, A. Walsh, T. G. Deutsch, Y. Yan, S.-H. Wei, J. A. Turner and M. M. Al-Jassim, unpublished.
- A. Janotti and C. G. Van de Walle, *Phys. Rev. B*, 2007, **76**, 165202.
- K. G. Godinho, A. Walsh and G. W. Watson, *J. Phys. Chem. C*, 2009, **113**, 439.
- F. A. Grant, *Rev. Mod. Phys.*, 1959, **31**, 646.
- M. N. Huda, Y. Yan, C. Y. Moon, S.-H. Wei and M. M. Al-Jassim, *Phys. Rev. B*, 2008, **77**, 195102.
- S. K. Deb, *Sol. Energy Mater. Sol. Cells*, 2008, **92**, 245.
- B. J. Morgan and G. W. Watson, *Surf. Sci.*, 2007, **601**, 5034.
- X. Nie, S.-H. Wei and S. B. Zhang, *Phys. Rev. Lett.*, 2002, **88**, 066405.
- L.-J. Shi, Z.-J. Fang and J. Li, *J. Appl. Phys.*, 2008, **104**, 073527.
- W. C. Sheets, E. S. Stampler, M. I. Bertoni, M. Sasaki, T. J. Marks, T. O. Mason and K. R. Poeppelmeier, *Inorg. Chem.*, 2008, **47**, 2696.
- H. Kawazoe, M. Yasukawa, H. Hyodo, M. Kurita, H. Yanagi and H. Hosono, *Nature*, 1997, **389**, 939.
- D. O. Scanlon, A. Walsh, B. J. Morgan, G. W. Watson, D. J. Payne and R. G. Eg dell, *Phys. Rev. B*, 2009, **79**, 035101.
- T. Arnold, D. J. Payne, A. Bourlange, J. P. Hu, R. G. Eg dell, L. F. J. Piper, L. Colakrol, A. De Masi, P.-A. Glans, T. Learmonth, K. E. Smith, J. Guo, D. O. Scanlon, A. Walsh, B. J. Morgan and G. W. Watson, *Phys. Rev. B*, 2009, **79**, 075102.
- R. Nagarajan, A. D. Draeseke, A. W. Sleight and J. Tate, *J. Appl. Phys.*, 2001, **89**, 8022.
- G. Li, D. Zhang and J. C. Yu, *Chem. Mater.*, 2008, **20**, 3983.
- I. C. Vinke, J. Diepgond, B. A. Boukamp, K. J. de Vries and A. J. Burggraaf, *Solid State Ionics*, 1992, **57**, 83.
- K. Sayama, A. Nomura, Z. Zou, R. Abe, Y. Abe and H. Arakawa, *Chem. Commun.*, 2003, 2908.
- A. Walsh, Y. Yan, M. N. Huda, M. M. Al-Jassim and S.-H. Wei, *Chem. Mater.*, 2009, **21**, 547.

-
- 69 A. Kudo, K. Omori and H. Kato, *J. Am. Chem. Soc.*, 1999, **121**, 11459.
- 70 D. J. Payne, R. G. Eggell, A. Walsh, G. W. Watson, J. Guo, P. A. Glans, T. Learmonth and K. E. Smith, *Phys. Rev. Lett.*, 2006, **96**, 157403.
- 71 A. Walsh and G. W. Watson, *J. Solid State Chem.*, 2005, **178**, 1422–1428.
- 72 Y. Ogo, H. Hiramatsu, K. Nomura, H. Yanagi, T. Kamiya, M. Hirano and H. Hosono, *Appl. Phys. Lett.*, 2008, **93**, 032113.
- 73 T. F. W. Barth and E. Posnjak, *Z. Kristallogr. Kristallgeom. Kristallphys. Kristallchem.*, 1934, **88**, 265.
- 74 A. Magneli, *Ark. Kem.*, 1941, **15**, 1.
- 75 A. Bystroem, B. Hoek and B. Mason, *Ark. Kem.*, 1942, **15**, 1.
- 76 E. E. Rodriguez, F. Poineau, A. Llobet, K. Czerwinski, R. Seshadri and A. K. Cheetham, *Inorg. Chem.*, 2008, **47**, 6281.
- 77 H. Mizoguchi and P. M. Woodward, *Chem. Mater.*, 2004, **16**, 5233.
- 78 Y. Hosogi, Y. Shimodaira, H. Kato, H. Kobayashi and A. Kudo, *Chem. Mater.*, 2008, **20**, 1299.